Removal of Pesticides from Aqueous Solutions Using Activated Carbon Derived from Jordanian Jift

Enas N. Mahmoud[1], Rafea Naffa[1], Khalil M. Ibrahim[2], Sawsan Jaafreh[1*], Manal H. Al-Bzour[1], Abdallah Abuferweh[1]

[1] Department of Chemistry, Faculty of Science, The Hashemite University, Zarqa 13133, Jordan
[2] Department of Earth and Environmental Sciences, Prince El-Hassan Bin Talal Faculty of Natural Resources and Environment, The Hashemite University, Zarqa 13133, Jordan

Corresponding Author Email: sawsan.jaafreh@hu.edu.jo

ABSTRACT

The widespread use of pesticides has led to significant contamination of both surface and groundwater, emerging as a critical environmental issue in recent years. One common method to remove pesticides from aqueous solutions is the adsorption process utilizing activated carbon. Here, the olive oil pomace (locally known as Jift) was used to prepare the activated carbon. The ability of the activated carbon prepared from Jift (ACJ) to remove several pesticides, including Metalaxyl, Imidacloprid, Methomyl, and Paraquat Dichloride, from aqueous solution was then investigated. The Jift was roasted and then activated by CO_2 at 800°C. ACJ was characterized by Scanning Electron Microscope, which shows that the pores in ACJ are mostly micropores. The specific surface area of ACJ and clay Jordanian minerals (Zeolite and Bentonite) was calculated using Methylene Blue (MB). Among these adsorbents, ACJ has the highest specific surface area (561.1 m^2/g), making it a promising adsorbent for pesticide removal. The uptake of pesticides using ACJ was compared with that of Zeolite and Bentonite. ACJ showed a high ability to remove all four pesticides, while Zeolite and Bentonite were only able to remove Paraquat Dichloride. The experimental data derived from the equilibrium adsorption isotherm were analyzed using the Langmuir and Freundlich models. The results indicated that the Langmuir model provided a superior fit to the data for the four pesticides, as evidenced by a high correlation coefficient ($R^2 > 0.95$) compared to the Freundlich model. Langmuir maximum adsorption capacity (q_m) were 277.30, 233.97, 119.71, and 74.94 mg/g for Methomyl, Imidacloprid, Metalaxyl, and Paraquat Dichloride, respectively. The Freundlich model was fitted only to the data for Methomyl and Imidacloprid ($R^2 > 0.96$). The heterogeneity factor ($1/n$) values for the two pesticides are less than unity, indicating a favorable adsorption process, and an increase in adsorption capacity. That explains why q_m of Methomyl and Imidacloprid were significantly higher than those of the other pesticides. The nature of the adsorption process was favorable for all four pesticides, as indicated by the estimated values of the Langmuir isotherm equilibrium parameter (R_L), which fell within the range of $0 < R_L < 1$. Two kinetic models (pseudo-first-order and pseudo-second-order) were used to assess the adsorption kinetic data. The pseudo-second-order model provided a better representation of the adsorption kinetics ($R^2 > 0.97$), which indicates that the adsorption process follows a chemisorption mechanism. These results demonstrate the potential of ACJ as an effective adsorbent for removing pesticides in water treatment applications.

1. INTRODUCTION

Jordan, a country in the Middle East, confronts a significant water scarcity crisis. This country has one of the lowest levels of water resources in the world and is considered to be among the most arid countries. Jordan currently supplies 150 m^3 of water per person annually, representing approximately one-third of the worldwide average. Water scarcity is attributable to the growing fluctuations in climate conditions, specifically concerning precipitation and rising temperatures. Furthermore, the issue has worsened due to the continuous large-scale refugee influx, exacerbating the population-water imbalance. Although there are some surface water resources available, Jordan's main supply of water is derived from harvested rainwater through various means such as rivers, dams, lakes, and groundwater. As a result, it is crucial to utilize treated wastewater in Jordan, particularly in the agriculture sector [1-3]. Consequently, approximately 95% of Jordan's wastewater is treated, with over 92% utilized in agricultural activities [4]. In Jordan, similar to many nations, the assessment of wastewater quality depends on the monitoring of standard parameters governed by the European Urban

Wastewater Directive (91/271/EEC). These metrics encompass phosphates, nitrates, chemical and biochemical oxygen demand, and total suspended solids. Nevertheless, some compounds that may present a risk to human health are not covered by these restrictions [2]. Recently, there has been wide documentation of the presence of emerging contaminants, such as pesticides, X-ray contrast media, personal care items, medicines, and endocrine disruptors in wastewater, surface waters, and groundwater [5].

Regarding pesticide contaminants, pesticides are recognized as agents that safeguard crops from harmful pests and diseases affecting humans. Their beneficial effects render pesticides an essential tool for maintaining and improving the quality of life for individuals across the globe. Each year, an average of two million tons of pesticides are utilized worldwide to combat weeds and pests. Pesticides are traditionally categorized based on the specific species they target including insecticides, herbicides, fungicides, rodenticides, and so forth [6]. The methods employed for the application of pesticides, such as spraying and spreading, can lead to their infiltration into soil and water systems in both agricultural and urban environments. The leaching of pesticides into groundwater is especially significant, given that groundwater serves as a crucial source for drinking water production. Consequently, pesticides adversely impact the environment [7, 8]. Pesticides are highly detrimental to human health, due to their toxicity, and being mutagenic, carcinogenic, and allergenic [9]. Pesticides have led to the widespread presence of pollution worldwide [10]. Therefore, there is an urgent need to remove residual pesticides from water systems.

Among various water-soluble pesticides, we selected, in this work, Metalaxyl, Imidacloprid, Methomyl, and Paraquat Dichloride as model pesticide pollutants. The selection of these pesticides was based on their high solubility in water, their existence in the Jordanian market, and their use by Jordanian farmers. These pesticides were obtained from the Jordanian factory VAPCO (Veterinary and Agricultural Products Manufacturing Company, Jordan) which is considered one of the largest factories in Jordan. The properties of these pesticides are shown in Table 1.

Table 1. Pesticides used in this study and their properties

Pesticide	Structure and Chemical Formula	Molecular Weight (g/mole)	Solubility in Water	References
Metalaxyl (97% Pure, Solid)	$C_{15}H_{21}NO_4$	279.3	7.9 g/L at 25°C	[11]
Imidacloprid (97% Pure, Solid)	$C_9H_{10}ClN_5O_2$	255.7	0.61 g/L at 20°C	[12]
Methomyl (98% Pure, Solid)	$C_5H_{10}N_2O_2S$	162.2	57.9 g/L at 25°C	[13]
Paraquat Dichloride (30.5% w/v, Solution)	$C_{12}H_{14}N_2Cl_2$	257.2	620 g/L at 20°C	[14]
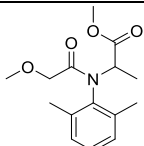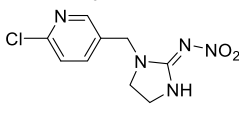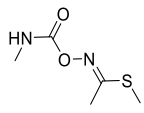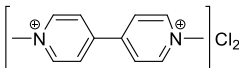
Metalaxyl is a fungicide used to suppress plant diseases [15, 16]. However, the significant solubility of Metalaxyl in water facilitates its leaching to groundwater and flow into waterways through agricultural runoffs. Accordingly, owing to its high residual levels in agricultural crops, Metalaxyl might lead to environmental hazards under natural conditions [16]. On the other hand, Imidacloprid ranks among the best-selling insecticides globally, and it is considerably effective in crop protection from pests [17]. Recent research has demonstrated that imidacloprid poses a toxic threat to humans, with acute toxicity potentially resulting in loss of consciousness and significant respiratory failure [18]. Additionally, Methomyl is an insecticide utilized in agriculture for crop protection. Nevertheless, the extensive use of this insecticide has caused human health issues and environmental toxicity. Methomyl is highly toxic to humans, and severe poisoning or death can result if exposed to high concentrations [13]. Based on the European Union pesticide regulations, Methomyl has been revoked as a recognized active ingredient; it can only be used by specially trained and certified applicators or under their direct supervision [19]. Finally, Paraquat Dichloride is a commonly utilized herbicide in agriculture to manage grassy weeds and broadleaf. Its herbicidal and toxicological properties are attributed to the presence of a diquaternary bipyridyl unit, whereas the chloride anions have few toxic effects [20]. The fatality rate of paraquat poisoning far surpasses that of other pesticide poisonings owing to its severe toxicity [21]. Due to its profound toxicity to humans, Paraquat use is prohibited in the European Union and restricted in the United States of America [20].

Developing various removal strategies for pesticides has motivated a new research drive in environmental remediation. Consequently, numerous techniques have been examined for the breakdown of pesticides, including biodegradation [22], adsorption [23-25], photocatalytic [26], electrochemical [27] processes, as well as nano-based techniques [28]. However, activated carbon adsorption remains the most effective and common method for the removal of pesticides from water

sources [29].

Activated carbon is widely recognized for its large surface area and significant adsorption capacity, high specific porosity, pore structure, customizable surface functionalization, and chemical and thermal stability. Furthermore, a variety of materials can be used to create activated carbon, including petroleum byproducts, biomass, coal, wood, polymers, and resins [30-33]. Additionally, activated carbon produced from biomass has received significant attention since it is considered to have an environmentally and economically friendly nature [30-32]. Moreover, activated carbon is notable for its low cost and simple operation [34]. Moreover, many researchers have studied adsorption of a wide range of pesticides from water using activated carbon as an adsorbent prepared from various biomass sources such as wheat straw [35], prickly pear seeds [9], peach stones [36], tea residue [37], pomegranate peels [38], cassava husks [39], strawberry seeds and pistachio shells [40], orange peels [41], and silkworm feces [42].

The present study focused on the investigation of pesticides adsorption on activated carbon prepared from Jift (the local name for olive oil pomace) [43]. With an approximate yearly production of 21.5×10^3 tons, olive oil is one of Jordan's most important agricultural products [44]. The olive oil extraction process produces olive oil (main product, 20%), moist solid waste (byproduct, 30%), and liquid waste (byproduct, 50%). Jift, which represents 65% of the moist solid waste, is a mixture of leftover pits and olive paste that is generated after the olives have been pressed [45]. Each year, Jordan produces around 50 - 60 thousand tons of olive Jift [45, 46].

Consequently, the primary aim of this research is to prepare and characterize activated carbon from Jordanian Jift (ACJ) and to investigate its efficiency for the removal of Metalaxyl, Imidacloprid, Methomyl, and Paraquat Dichloride pesticides from water. These pesticides were chosen to be investigated in this study because of their toxic nature and significant solubility in water. Additionally, the efficiency of ACJ was compared with that of some commercial adsorbents. These adsorbents include Bentonite and Zeolite. After the characterization of different adsorbents, a study was performed to assess the effectiveness of removing these pesticides from aqueous solutions. This research aimed to address two significant waste issues in Jordan: harmful pesticides and Jift.

2. MATERIALS AND METHODS

2.1 Chemicals

Metalaxyl, Imidacloprid, Methomyl, and Paraquat Dichloride pesticides were used in this study. These pesticides were obtained in solid form from VAPCO industry with a purity ranging from 97% - 98% except for Paraquat Dichloride which was obtained in a solution form with a concentration of 30.5% w/v. All pesticides were used as received. The pesticides and chemicals utilized in this study are detailed in Table 2.

Table 2. Chemicals utilized in this work

Material	Grade	Source	Note
Distilled Water	-	The Hashemite University	pH = 5.3 - 6.5
Methylene Blue Trihydrate	Analytical	Scharlau	Hydrated water is lost on drying at 110°C
Metalaxyl	Technical	VAPCO	97% pure
Imidacloprid	Technical	VAPCO	97% pure
Methomyl	Technical	VAPCO	98% pure
Paraquat Dichloride	Technical	VAPCO	30.5% w/v
Sodium Dithionite	Analytical	VAPCO	-
Acetonitrile	HPLC	VAPCO	-
HPLC Water	HPLC	VAPCO	-
N_2 gas	Analytical	Jordanian Gas Company	98% - 99%
CO_2 gas	Analytical	Jordanian Gas Company	92% - 96%

2.2 Equipment

Thermostatic Shakers and Baths: A Julabo GLF 1083 thermostatic water bath shaker was used, and its temperature was controlled within ± 0.2°C and kept at 25°C. pH-Meter: All pH measurements of samples were carried out using 420A Orion pH meter with a combination of glass electrode with an accuracy of ± 0.005 pH units. Ultrasonic Shaker: All solids were dissolved using 5510 Branson ultrasonic shaker with a constant frequency of 42 kHz. UV-Visible Spectrophotometer: Absorbance measurements were carried out using a Cary 100 Bio Spectrophotometer, and the wavelength accuracy was within ± 0.2 nm. Furnaces: Activated carbon was prepared by using a Thermolyne 47900 furnace, and the temperature accuracy was within ± 2°C. High Performance Liquid Chromatography (HPLC): The instrument was located in the VAPCO Factory, and the system includes a Merck and Hitachi series D-6200A. Centrifuge: Adsorbents were separated from solutions using Z 200A Hermel centrifuge, with rotational speed ranging from 100 rpm to 6000 rpm and with a timer range from 1 min up to 60 min. Scanning Electron Microscope (SEM): Adsorbents' surface characterization was done using a SEM FEI Model Quanta 200, and the coating machine was a Polaron E 6100 using a Vacuum Coater with gold disk (sputtering method) at 1200 V and 20 mA.

2.3 Analysis of pesticides

The analysis of Metalaxyl, Imidacloprid and Methomyl was carried out using HPLC as illustrated in Table 3, whereas Paraquat Dichloride was converted to a complex with sodium dithionite to obtain an absorption curve in the visible region. The stock solution for the calibration curve of Paraquat Dichloride was prepared by mixing 100 mL of a 100 ppm Paraquat Dichloride solution with a freshly prepared 1% sodium dithionite solution in 1 M NaOH. The absorbance was measured using a UV spectrophotometer at the maximum wavelength (λ_{max}) of 600 nm.

Table 3. HPLC conditions for pesticides analysis

Pesticide	Mobile Phase (Acetonitrile: Water)	λ_{max} (nm)	Concentration Working Range (ppm)	Retention Time (min)
Metalaxyl	60 : 40	236	10 - 50	2.99 ± 0.20
Imidacloprid	60 : 40	274	5 - 40	3.23 ± 0.20
Methomyl	80 : 20	267	50 - 500	3.95 ± 0.20

2.4 Adsorbents preparation

2.4.1 Collection and preparation of Zeolite and Bentonite

Zeolite was collected from Jabal Hannoun which is approximately 180 km northeast of Amman. Whereas Bentonite was collected from Ein-Al Bayda and Qa'a Al-Azraq that are approximately 120 km northeast of Amman. Both clay samples were ground using an agate mortar, and particles larger than 147 μm were removed by sieving with a CISA sieve St. (ISO 3310.1). Only those that passed the 147 μm sieve were used in the present investigation.

2.4.2 Collection and preparation of Jift raw samples

Raw Jift samples were collected from an olive mill press company in Al-Zarqa city, Jordan. The samples were dried in a large open area for 15 days to ensure complete drying. The samples were subsequently processed through mechanical grinding, and particles larger than 1 mm were removed through sieving. Only those that passed the 1 mm sieve were used in the following experiment.

2.4.3 Preparation of roasted Jift

The ground Jift samples ($\leq$ 1 mm) were roasted in an iron pan for approximately 30 min until all the Jift was converted to black ash. The black ash was sieved through a 147 μm, and only those passing the sieve were used in the following experiment.

2.4.4 Preparation of activated carbon from Jift (ACJ)

To hold the roasted Jift sample inside the furnace, a laboratory-scale iron box reactor was designed and manufactured by the engineering workshops of The Hashemite University. Figure 1 shows a schematic diagram of the experimental setup of the reactor-furnace systems used in this research.
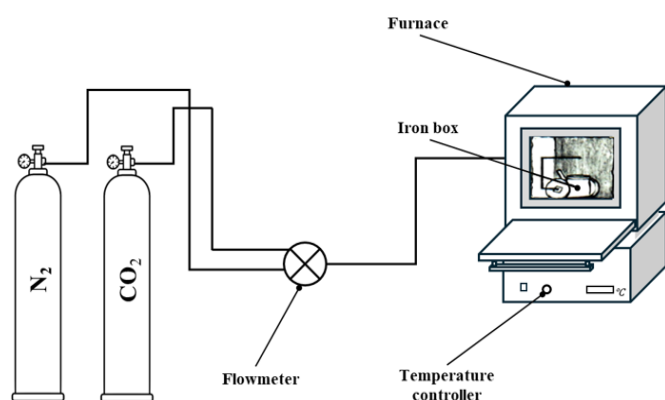
Figure 1. Reactor-Furnace system setup

A 50 g sample of roasted Jift ($\leq$ 147 μm) was placed in the reactor-furnace. To ensure an oxygen free atmosphere during temperature elevation, N_2 gas was pumped into the reactor for 15 min before heating, then the temperature increased to 600°C, while the N_2 gas flow kept continuous. Subsequently, the sample was kept under the N_2 atmosphere for half an hour.

After that, the temperature was raised to 800°C and the N_2 gas was replaced with a continuous flow of CO_2 gas for one hour at the same temperature [47]. Then, the furnace was turned off while continuous CO_2 gas kept flowing for another hour. Subsequently, the gas flow was turned off and the sample was left in the furnace to cool for 3 hours, and it was then transferred to a desiccator to cool overnight. Finally, the sample was ground gently in an agate mortar and sieved. Only particles that passed through the 147 μm sieve were utilized in the subsequent analyses.

2.5 Batch adsorption isotherm

Isotherm models are commonly employed to illustrate the equilibrium of the bio-sorption process, with experimental data being fitted to models such as Langmuir and Freundlich. In this work, we applied the Langmuir and Freundlich models which are represented in linear form as in Eq. (1) and Eq. (2), respectively [48, 49].

$$\frac{C_e}{q_e} = \frac{C_e}{q_m} + \frac{1}{K_L q_m} \qquad (1)$$

$$log\, q_e = \frac{1}{n} log\, C_e + log\, K_F \qquad (2)$$

where, C_e is the equilibrium concentration of adsorbate in the solution (mg/L), q_e is the adsorption capacity at equilibrium (mg/g), q_m is the maximum adsorption capacity (mg/g), K_L is the Langmuir constant (L/mg), K_F is the Freundlich constants related to adsorption capacity ($[mg/g]\,[L/mg]^{1/n}$), n is a constant which gives an idea of the grade of heterogeneity, and 1/n is the heterogeneity factor. The equilibrium concentration of adsorbate (q_e), which appears in both Eq. (1) and Eq. (2), can be calculated using Eq. (3) [48]:

$$q_e = \frac{(C_0 - C_e) \times V}{m} \qquad (3)$$

where, C_0 is the adsorbate initial concentration (mg/L), V is the sample volume (L), and m is the mass of the dry adsorbent (g).

Langmuir model posits that adsorption happens only at a limited number of specific localized locations, resulting in a monolayer adsorption, where the adsorbed layer is a single-molecule-thick of adsorbate [50]. Meanwhile, Freundlich isotherm describes the process of multilayer and heterogeneous adsorption on the surface of the adsorbent [51].

The fundamental properties of the Langmuir isotherm can be expressed through a dimensionless constant known as the equilibrium parameter (R_L), which is calculated as indicated in Eq. (4) [52]:

$$R_L = \frac{1}{(1 + K_L C_0)} \qquad (4)$$

The values of R_L indicate the nature of the adsorption

process [52]. For instance, the adsorption process is unfavorable if $R_L > 1$. While the adsorption process is linear if $R_L = 1$. Whereas the adsorption process is favorable if the value lies between 0 and one ($0 < R_L < 1$). On the other hand, the adsorption process is irreversible if $R_L = 0$.

In this study we used the isotherm models to evaluate the specific surface area of roasted Jift, ACJ, Bentonite, and Zeolite adsorbents. Furthermore, the isotherm models were employed to assess the q_m for the pesticides (Metalaxyl, Imidacloprid, Methomyl, and Paraquat Dichloride) on ACJ.

To guarantee the reliability of the data for the ensuing experiments, both blank and control samples were simultaneously prepared and processed for each adsorption test. A blank sample composed of the adsorbent and distilled water in a screw-cap flask devoid of any adsorbate. While the control sample consisted of adsorbate in a screw-cap flask without any adsorbent.

2.5.1 Specific surface area

The determination of specific surface area for activated carbon by the adsorption of Methylene Blue (MB) in liquid phase has been adopted widely [53]. In order to determine the specific surface area of adsorbents (Roasted Jift, ACJ, Bentonite, and Zeolite), we employed MB as adsorbate, and the data were analyzed using the Langmuir mode.

The subsequent formula was used to determine the specific surface area [53]:

$$S_{MB} = \frac{q_m \times A_{MB} \times N_A \times 10^{-20}}{M} \quad (5)$$

where, S_{MB} is the specific surface area in m^2/g, q_m is the maximum number of molecules of MB adsorbed at the monolayer of adsorbent in mg/g (obtained from Eq. (1)), A_{MB} is the occupied surface area of one molecule of MB = 120 Å^2 [54], N_A is Avogadro's number = 6.02×10^{23} mol^{-1}, and M is

the molar weight of MB = 319.85×10^3 mg/mol.

S_{MB} for four different adsorbents (Roasted Jift, ACJ, Bentonite, and Zeolite) were calculated based on the MB adsorption isotherm. Different weights of adsorbents ranging from (0.02 - 0.2 g) were mixed with 50 mL of MB (100 ppm with Roasted Jift, 500 ppm with ACJ, 250 ppm with Bentonite, and 100 ppm with Zeolite) in 100 mL screw-cap flasks. To achieve equilibrium, the flasks were shaken overnight at 25°C [55]. Following this, the suspension was filtered and, when necessary, diluted to achieve the desired concentration. Subsequently, a UV-Visible spectrophotometer was employed to determine the concentration of MB at its peak wavelength of 664 nm [56].

2.5.2 Pesticides uptake

The pesticides uptake was measured using three adsorbents (ACJ, Bentonite, and Zeolite) by using certain weight from each adsorbent. The adsorbents were mixed with a 50 mL of Metalaxyl, Imidacloprid, Methomyl, and Paraquat Dichloride in 100 mL screw-cap flasks. The weight of adsorbents and pesticides concentration are summarized in Table 4. In order to attain equilibrium, the flasks were shaken overnight at 25°C. The suspension was subsequently filtered and diluted as required. Then, the analysis of Pesticides was carried out as mentioned before in section 2.3 (Analysis of Pesticides).

2.5.3 Maximum adsorption capacity (q_m)

q_m was calculated for ACJ by utilizing different weights of adsorbent ranging from (0.02 - 0.2 g). The ACJ was mixed with a 50 mL of Metalaxyl (500 ppm), Imidacloprid (500 ppm), Methomyl (500 ppm), and Paraquat Dichloride (200 ppm) in 100 mL screw-cap flasks. To establish equilibrium, the flasks were shaken overnight at 25°C. The suspension was subsequently filtered and diluted if deemed necessary. Then, the analysis of Pesticides was carried out as mentioned before in section 2.3 (Analysis of Pesticides).

Table 4. The adsorption capacity

Pesticide	Pesticide Concertation (ppm)			Adsorbent Weight (g)		
	ACJ	Bentonite	Zeolite	ACJ	Bentonite	Zeolite
Metalaxyl	500	50	50	0.13	2.00	2.00
Imidacloprid	500	50	50	0.13	2.00	2.00
Methomyl	500	50	50	0.13	2.00	2.00
Paraquat Dichloride	200	200	200	0.13	0.20	0.30

2.6 Batch kinetic study

Batch kinetic study was performed for Pesticides adsorption on ACJ. The concentration of Metalaxyl, Imidacloprid, and Methomyl was 500 ppm. Ultrasonication was used to dissolve the pesticides at room temperature. While Paraquat Dichloride pesticide solution had a concentration of 200 ppm. All solutions were freshly prepared for each run. Fourteen samples from each pesticide were prepared by adding 50 mL of the pesticide solution to a fixed mass of 0.1 g of ACJ in 100 mL screw-cap flask. Each sample was prepared in duplicate. All flasks were put in a thermostat shaker at 25°C. After appropriate time intervals (1, 5, 10, 15, 20, 30, 60, 120, 180, 240, 300, 360, 480, and 1440 min), the samples were centrifuged, filtered, and the clear solution was analyzed for pesticide concentration as mentioned before in section 2.3 (Analysis of Pesticides). Two additional samples from each pesticide were prepared using the previously mentioned procedure. These samples were put in a thermostat shaker for

1440 min (24 hours) to allow the adsorption process to reach equilibrium.

3. RESULTS AND DISCUSSION

3.1 Characterization

The production of activated carbon can be achieved by two methods: physical activation with oxidizing agents such as steam or CO_2, and chemical activation with mineral salts [57]. In this study, physical activation for Jift was selected. CO_2 was chosen as the activation gas due to its cleanliness and ease of handling. Furthermore, CO_2 is often selected as the activation gas on the laboratory scale, as it allows for enhanced control over the activation process owing to its low reaction rate at temperatures near 800°C [58]. Before the activation process, the ground Jift samples (≤ 1 mm) were roasted. According to Zhao et al. [59], roasting of biomass increased its

hydrophobicity, and can effectively reduce its moisture content. The features of roasted Jift and ACJ were characterized as follows:

3.1.1 Scanning Electron Microscopy (SEM)

SEM is extensively utilized to investigate the morphology and surface characteristics of the adsorbent materials. Figure 2 and Figure 3 present the SEM micrographs for the roasted Jift and ACJ, respectively.

Figure 2 shows that the roasted Jift has an almost smooth surface with very low micropores. This is probably due to the lack of the activation step responsible for pore growth at the surface. On the other hand, Figure 3 shows that the ACJ is mostly microporous with low mesopores. This is consistent with the findings of Wang et al. [60], who mentioned that activated carbon is mainly a microporous solid, but it also contains mesopores and macropores.
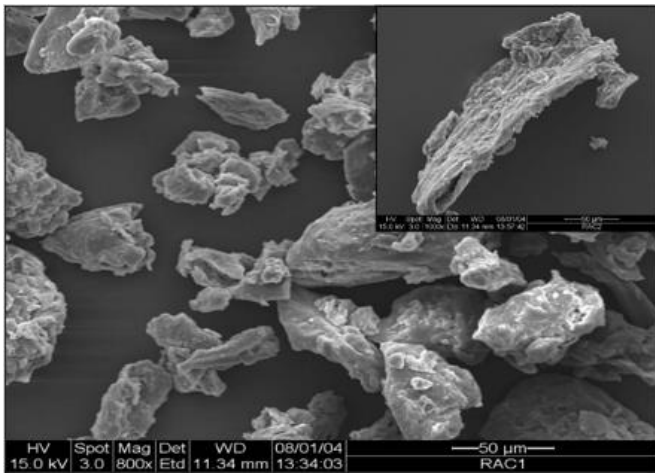
Figure 2. SEM for roasted Jift
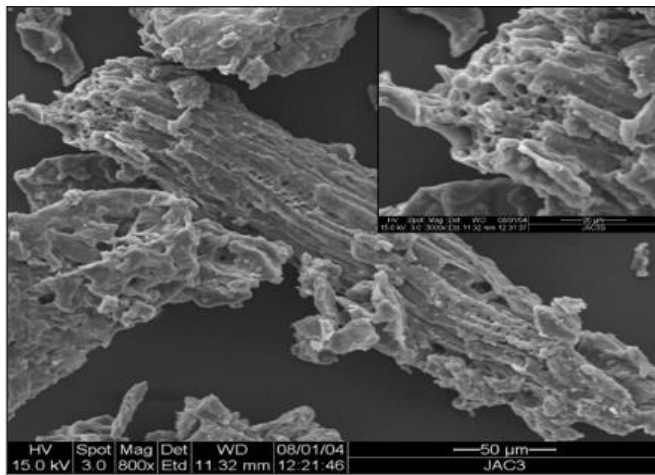
Figure 3. SEM for the ACJ

3.1.2 Specific surface area by Methylene Blue (MB)

In addition to roasted Jift and ACJ, the specific surface area was measured for commercial adsorbents (Bentonite and Zeolite). This measure was implemented for comparison. The data obtained for the adsorption of MB by the adsorbents were analyzed using Langmuir adsorption isotherms model (Eq. (1)). The values of q_m for MB and the correlation coefficient are listed in Table 5.

Using the calculated q_m values listed in Table 5, the specific surface areas (S_{MB}) were calculated using Eq. (5), and the

results are shown in Figure 4.

Table 5. The maximum adsorption capacity of MB

Adsorbent	q_m (mg/g)	R^2
Roasted Jift	130.6	0.9863
ACJ	248.4	0.9913
Bentonite	203.2	0.9984
Zeolite	124.4	0.9967
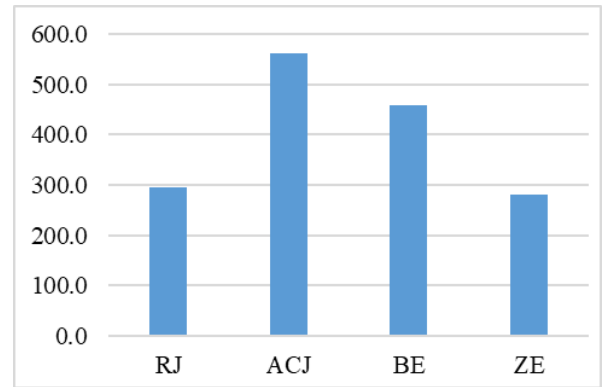
Figure 4. Specific surface area (m^2/g) for all adsorbents using MB adsorption methods, where RJ, ACJ, BE, and ZE refers to the roasted Jift, ACJ, Bentonite, and Zeolite, respectively

The findings indicate that the ACJ exhibits a greater specific surface area when compared to the roasted Jift, which aligns with the results obtained from the SEM analysis. The physical activation process of biomass (carbon surface) with CO_2 proceeds via a certain reaction (Eq. (6)), which increases the porosity of the surface resulting in a larger surface area [31, 61].

$$C_{(S)} + CO_{2(g)} \rightarrow 2CO_{(g)} \tag{6}$$
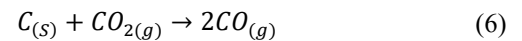
Furthermore, the ACJ has the highest specific surface area (561 m^2/g) compared with the used commercial adsorbents; such that ACJ > Bentonite > Zeolite. Compared to literature, the same arrangement was found [62, 63].

3.2 Pesticides uptake

The uptake of Metalaxyl, Imidacloprid, Methomyl, and Paraquat Dichloride by ACJ was evaluated using the adsorption capacity (q_e), which was calculated using Eq. (3). Promising results were obtained for the removal of the pesticides from aqueous solutions demonstrating that the ACJ has a high ability to remove the pesticides. For each pesticide, one gram of ACJ was able to adsorb around 161 mg of Methomyl, 151 mg of Imidacloprid, 119 mg of for Metalaxyl, and 70 mg of Paraquat Dichloride (see Table 6).

The q_e of ACJ was compared with that of clay Jordanian minerals (Zeolite and Bentonite), and the results are listed in Table 6. The results shows that the Zeolite and Bentonite are disabled to remove the Metalaxyl, Imidacloprid, and Methomyl. While for Paraquat Dichloride, the ACJ has the largest adsorption capacity followed by Bentonite, and the Zeolite has the lowest value. These results agreed with the measured specific surface area shown in Figure 4. ACJ shows promising results for removing all four pesticides from aqueous solutions, this may arise from the ability of the ACJ

surface to form π-π associations with pesticides [64]. While Zeolite and Bentonite demonstrate predictable behavior attributable to their inorganic cation content, which becomes highly hydrated in aqueous solutions. This hydration confers a hydrophilic quality to their surfaces, facilitating the adsorption of polar or ionic compounds. Conversely, these materials are not suitable for the adsorption of hydrophobic or non-ionic organic substances [65, 66].

Table 6. The adsorption capacity at equilibrium

Pesticide	q_e (mg/g)		
	ACJ	Bentonite	Zeolite
Metalaxyl	119.030	0.838	0.000
Imidacloprid	151.220	0.450	0.100
Methomyl	160.740	1.175	0.225
Paraquat Dichloride	70.280	49.500	21.000

3.3 Adsorption isotherm of pesticide over ACJ

To investigate the relationship between the adsorbate (Metalaxyl, Imidacloprid, Methomyl, and Paraquat Dichloride) and ACJ at equilibrium, different adsorption isotherm models were employed to interpret the experimental data. The Langmuir and Freundlich models were investigated in this study. As seen in Figure 5 and Figure 6, Langmuir provides a better fitting than the Freundlich mode.

The calculated parameters for the adsorption isotherm models are listed in Table 7. The linear plotting of C_e/q_e versus C_e in Langmuir model gives high correlation coefficient ($R^2 > 0.95$) for all pesticides, which indicates monolayer adsorption. The highest Langmuir maximum adsorption capacity (q_m) was for Methomyl (277.30 mg/g), due to its low molecular weight compared to the other pesticides investigated in this study. This finding aligns with Cougnaud et al. [67], who reported that a decrease in pesticide molecular weight generally results in an increase in q_m. While the q_m order for the other pesticides is Imidacloprid > Metalaxyl > Paraquat Dichloride. This order indicates that the q_m of pesticides was inversely related to their water solubility. A similar behavior was also observed by Faur et al. [68]. It is also notable that the maximum adsorption capacity of Methomyl (277.30 mg/g) and Imidacloprid (233.97 mg/g) are considerably greater than those of Metalaxyl (119.71 mg/g) and Paraquat Dichloride (74.94 mg/g), which could be explained by the Freundlich model. This model was only fitted to the data for Methomyl and Imidacloprid. The linear correlation between Log q_e and Log

C_e (Figure 6) for these two pesticides exhibits a high correlation coefficient ($R^2 > 0.96$). The parameters derived from the Freundlich model are detailed in Table 7. The calculated $1/n$ values for Methomyl and Imidacloprid are less than unity, which indicates that the adsorption process for these pesticides is favorable, with available new adsorption sites and an increase in adsorption capacity [69].
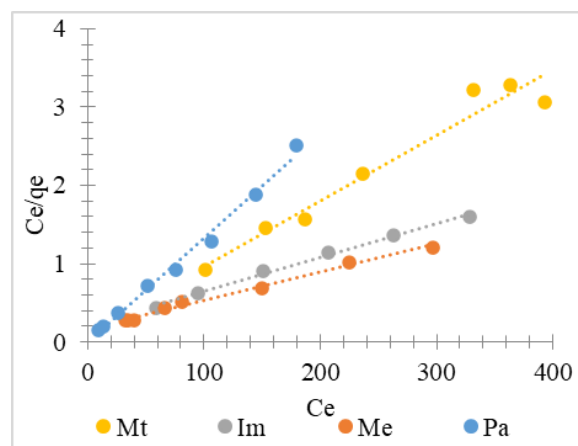
Figure 5. Adsorption Langmuir isotherm model, where Mt, Im, Me, and Pa refers to Metalaxyl, Imidacloprid, Methomyl, and Paraquat Dichloride, respectively
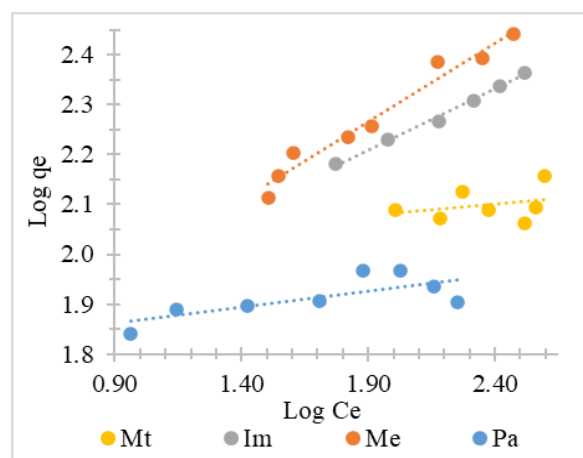
Figure 6. Adsorption Freundlich isotherm model, where Mt, Im, Me, and Pa refers to Metalaxyl, Imidacloprid, Methomyl, and Paraquat Dichloride, respectively

Table 7. Adsorption isotherm models parameter

Pesticide	Langmuir Adsorption Isotherm			Freundlich Adsorption Isotherm		
	q_m (mg/g)	K_L (L/mg)	R^2	$1/n$	K_F ([mg/g] [L/mg]$^{1/n}$)	R^2
Metalaxyl	119.71	0.0625	0.9537	0.0444	87.86	0.0878
Imidacloprid	233.97	0.0189	0.9935	0.2436	49.66	0.9937
Methomyl	277.30	0.0213	0.9921	0.3157	41.27	0.9679
Paraquat Dichloride	74.94	-1.6406	0.9910	0.0659	56.46	0.5469

To determine the nature of the adsorption process, the Langmuir isotherm equilibrium parameter (R_L) for the adsorption of the pesticides was calculated from Eq. (4). R_L values for the uptake of Metalaxyl, Imidacloprid, Methomyl, and Paraquat Dichloride are 1.68×10^{-5}, 8.62×10^{-6}, 7.27×10^{-6} and 6.43×10^{-5}, respectively, which reflect a favorable adsorption for the four pesticides.

3.4 Kinetic of pesticides removal

The adsorption Kinetic characteristics of pesticides by ACJ are shown in Figure 7. Metalaxyl, Methomyl, and Paraquat Dichloride have almost the same adsorption behavior, they show two distinct stages. The initial stage demonstrates a rapid surge in adsorption capacity (q_t), ensued by a more modest

rise. At the end of the first stage (~ 20 min) the adsorption capacity (in mg/g) for Metalaxyl, Methomyl, and Paraquat Dichloride increases up to 95.8, 185.9, and 40.9, respectively. After approximately 20 min, the second stage starts. The adsorption capacities for the three pesticides show a tiny increase with time until it reaches the equilibrium. The equilibrium adsorption capacity (in mg/g) for Metalaxyl, Methomyl, and Paraquat Dichloride are 132.40, 208.35, and 84.40, respectively. On the other hand, the adsorption process of Imidacloprid shows a different behavior. The adsorption capacity of Imidacloprid gradually increases over time, reaching 184.2 mg/g at approximately 360 minutes, which is a relatively long time compared to the other pesticides. While at equilibrium the adsorption capacity of Imidacloprid was 189.35 mg/g. The equilibrium stage for all pesticides is explained by the decline in the number of active adsorption sites on ACJ with time [70].
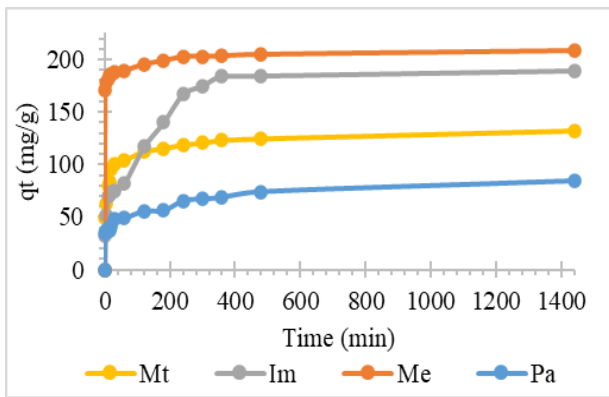
Figure 7. Adsorption capacity of pesticides versus time, where Mt, Im, Me, and Pa refer to Metalaxyl, Imidacloprid, Methomyl, and Paraquat Dichloride, respectively

In the present investigation, the Lagergren kinetic models (pseudo-first-order and pseudo-second-order) were utilized to elucidate the mechanism governing the adsorption process. The pseudo-first-order kinetic model of Lagergren is represented by Eq. (7) [71]:

$$log(q_e - q_t) = log\, q_{1e} - 2.303 K_1 t \qquad (7)$$

where, q_e and q_t are the amounts of pesticide adsorbed on ACJ (mg/g) at equilibrium and at time t (min), respectively, while q_{1e} is the calculated amounts of pesticide adsorbed on ACJ (mg/g) at equilibrium, and K_1 is the rate constant of pseudo-first-order adsorption (min^{-1}). The slope and intercept of the plot of Log (q_e-q_t) versus t were used to determine K_1 and q_{1e}. On the other hand, the pseudo-second-order kinetic model of Lagergren is expressed by Eq. (8) [70]:

$$\frac{t}{q_t} = \frac{1}{K_2 q_{2e}^2} + \frac{1}{q_{2e}} t \qquad (8)$$

where, q_{2e} is the calculated amounts of pesticide adsorbed on ACJ (mg/g) at equilibrium, and K_2 is the rate constant of pseudo-second-order adsorption (g.mg^{-1}.min^{-1}). The slope and intercept of the plot of t/q_t versus t are used to calculate q_{2e} and K_2. The adsorption rate constant and the calculated amounts of pesticide adsorbed on ACJ (K_1, K_2, q_{1e} and q_{2e}) along with correlation coefficients for the pseudo-first-order and pseudo-second-order Lagergren model are shown in Table 8.

Comparing the results shown in Table 8, the pseudo-second-order adsorption mechanism demonstrates the most favorable alignment with the data, as indicated by high correlation coefficient values ($R^2 > 0.97$). Additionally, a pseudo-second-order kinetic model is found to have a greater agreement between the computed (q_{2e}) and experimental (q_e) values than the pseudo-first-order kinetic model. This result indicates that the adsorption process is a chemisorption mechanism [72]. Similar kinetic results were reported for the adsorption of various pesticides by activated carbon prepared from orange peel [41] and silkworm feces [42].

Table 8. The parameter of kinetic model and the experimental q_e

Pesticide	q_e (mg/g)	Pseudo-First-Order			Pseudo-Second-Order		
		K_1 (min^{-1})	q_{1e} (mg/g)	R^2	K_2 (g.mg^{-1}.min^{-1})	q_{2e} (mg/g)	R^2
Metalaxyl	132.40	9.84×10^{-8}	48.33	0.8696	9.81×10^{-4}	125.29	0.9992
Imidacloprid	189.35	1.65×10^{-7}	147.58	0.9676	1.35×10^{-4}	194.61	0.9757
Methomyl	208.35	1.03×10^{-7}	25.97	0.9374	1.30×10^{-7}	204.90	0.9999
Paraquat Dichloride	84.40	6.79×10^{-8}	45.54	0.9748	7.41×10^{-4}	72.83	0.9898

4. CONCLUSION

In the present work adsorption of pesticides on ACJ was studied. ACJ was characterized by SEM and Specific Surface Area. Compared with Zeolite and Bentonite (their surface has a hydrophilic character), ACJ has the highest Specific Surface Area making it a promising candidate for pesticide adsorption, this may be due to the possibility to form π-π associations between the ACJ surface and pesticides. Furthermore, pesticides uptake using ACJ were compared with that of Zeolite and Bentonite, with ACJ showing a much higher ability to remove for all four pesticides. The Langmuir model provided a more accurate representation of the adsorption isotherm for all pesticides examined. Langmuir maximum adsorption capacity (q_m) were 277.30, 233.97, 119.71, and 74.94 mg/g for Methomyl, Imidacloprid, Metalaxyl, and Paraquat Dichloride, respectively. While Freundlich isotherm model was only fit to the data for Methomyl and Imidacloprid with heterogeneity factor values less than unity, indicating a favorable adsorption process, an increase in adsorption capacity for these pesticides. The nature of the adsorption process was favorable for the four pesticides, as indicated by Langmuir isotherm equilibrium parameter (R_L). Kinetics and equilibrium studies were also performed and they demonstrated that the pseudo-second-order model fits all four pesticides better, suggesting that the adsorption mechanism is chemisorption. The ACJ, being both cost-effective and simple to prepare, demonstrates a significant capacity to adsorb four different pesticides from aqueous solutions, which may increase its applicability in wastewater treatment processes. Nevertheless, to confirm the results and implement this technique on an industrial scale; more research using different

kinds of pesticides, actual wastewater samples, and the reuse of the ACJ bio-sorbent are needed.

REFERENCES

[1] Akkam, Y., Omari, D., Alhmoud, H., Alajmi, M., Akkam, N., Aljarrah, I. (2023). Assessment of xenoestrogens in Jordanian water system: Activity and identification. Toxics, 11(1): 63. https://doi.org/10.3390/toxics11010063

[2] Abu-Shmeis, R.M., Tarawneh, I.N., Al-Qudah, Y.H., Dabaibeh, R.N., Tarawneh, M.N. (2020). Evaluation of the removal efficiency of PCBs from five wastewater treatment plants in Jordan. Water, Air, & Soil Pollution, 231: 114. https://doi.org/10.1007/s11270-020-04482-5

[3] Al-Addous, M., Bdour, M., Alnaief, M., Rabaiah, S., Schweimanns, N. (2023). Water resources in Jordan: A review of current challenges and future opportunities. Water, 15(21): 3729. https://doi.org/10.3390/w15213729

[4] Al-Mashaqbeh, O., Alsafadi, D., Dalahmeh, S., Bartelt-Hunt, S., Snow, D. (2019). Removal of selected pharmaceuticals and personal care products in wastewater treatment plant in Jordan. Water, 11(10): 2004. https://doi.org/10.3390/w11102004

[5] Kumar, R., Qureshi, M., Vishwakarma, D.K., Al-Ansari, N., Kuriqi, A., Elbeltagi, A., Saraswat, A. (2022). A review on emerging water contaminants and the application of sustainable removal technologies. Case Studies in Chemical and Environmental Engineering, 6: 100219. https://doi.org/10.1016/j.cscee.2022.100219

[6] Syafrudin, M., Kristanti, R.A., Yuniarto, A., Hadibarata, T., et al. (2021). Pesticides in drinking water—A review. International Journal of Environmental Research and Public Health, 18(2): 468. https://doi.org/10.3390/ijerph18020468

[7] Swartjes, F.A., Van der Aa, M. (2020). Measures to reduce pesticides leaching into groundwater-based drinking water resources: An appeal to national and local governments, water boards and farmers. Science of the Total Environment, 699: 134186. https://doi.org/10.1016/j.scitotenv.2019.134186

[8] Araya, G., Perfetti-Bolaño, A., Sandoval, M., Araneda, A., Barra, R.O. (2024). Groundwater leaching potential of pesticides: A historic review and critical analysis. Environmental Toxicology and Chemistry, 43(12): 2478-2491. https://doi.org/10.1002/etc.5869

[9] Zgolli, A., Souissi, M., Dhaouadi, H. (2024). Purification of pesticide-contaminated water using activated carbon from prickly pear seeds for environmentally friendly reuse in a circular economy. Sustainability, 16(1): 406.

https://doi.org/10.3390/su16010406

[10] da Paixão Cansado, I.P., Mourão, P.A.M., Belo, C.R. (2022). Using Tectona Grandis biomass to produce valuable adsorbents for pesticide removal from liquid effluent. Materials, 15(17): 5842. https://doi.org/10.3390/ma15175842

[11] Vergili, I., Barlas, H. (2009). Removal of 2, 4-D, MCPA and Metalaxyl from water using Lewatit VP OC 1163 as sorbent. Desalination, 249(3): 1107-1114. https://doi.org/10.1016/j.desal.2009.06.043

[12] Yari, K., Rahmani, A., Asgari, G., Azarian, Q., Bhatnagar, A., Leili, M. (2017). Degradation of imidacloprid pesticide in aqueous solution using an eco-friendly electrochemical process. Desalination and Water Treatment, 86: 150-157. https://doi.org/10.5004/dwt.2017.21330

[13] Lin, Z., Zhang, W., Pang, S., Huang, Y., Mishra, S., Bhatt, P., Chen, S. (2020). Current approaches to and future perspectives on methomyl degradation in contaminated soil/water environments. Molecules, 25(3): 738. https://doi.org/10.3390/molecules25030738

[14] Teutli-Sequeira, A., Vasquez-Medrano, R., Prato-Garcia, D., Ibanez, J.G. (2020). Solar photo-assisted degradation of bipyridinium herbicides at circumneutral pH: A life cycle assessment approach. Processes, 8(9): 1117. https://doi.org/10.3390/pr8091117

[15] Wang, W., Liu, X., Han, T., Li, K., Qu, Y., Gao, Z. (2020). Differential potential of Phytophthora capsici resistance mechanisms to the fungicide Metalaxyl in peppers. Microorganisms, 8(2): 278. https://doi.org/10.3390/microorganisms8020278

[16] Hamed, S.M., Hassan, S.H., Selim, S., Wadaan, M.A., Mohany, M., Hozzein, W.N., AbdElgawad, H. (2020). Differential responses of two cyanobacterial species to R-metalaxyl toxicity: Growth, photosynthesis and antioxidant analyses. Environmental Pollution, 258: 113681. https://doi.org/10.1016/j.envpol.2019.113681

[17] Nugnes, R., Russo, C., Orlo, E., Lavorgna, M., Isidori, M. (2023). Imidacloprid: Comparative toxicity, DNA damage, ROS production and risk assessment for aquatic non-target organisms. Environmental Pollution, 316: 120682.
https://doi.org/10.1016/J.ENVPOL.2022.120682

[18] Shareefdeen, Z., Elkamel, A. (2024). Toxic and environmental effects of neonicotinoid based insecticides. Applied Sciences, 14(8): 3310. https://doi.org/10.3390/APP14083310

[19] Liang, C.A., Chang, S.S., Chen, H.Y., Tsai, K.F., et al. (2023). Human poisoning with methomyl and cypermethrin pesticide mixture. Toxics, 11(4): 372. https://doi.org/10.3390/toxics11040372

[20] Vasca, E., Siano, F., Caruso, T. (2023). Fluorescence detecting of paraquat and diquat using host-guest chemistry with a fluorophore-pendant calix [6] arene. Sensors, 23(3): 1120. https://doi.org/10.3390/s23031120

[21] Liu, X., Yang, H., Liu, Z. (2022). Signaling pathways involved in paraquat-induced pulmonary toxicity: Molecular mechanisms and potential therapeutic drugs. International Immunopharmacology, 113: 109301. https://doi.org/10.1016/j.intimp.2022.109301

[22] Jia, Z., Li, Y., Lu, S., Peng, H., Ge, J., Chen, S. (2006). Treatment of organophosphate-contaminated wastewater by acidic hydrolysis and precipitation. Journal of Hazardous Materials, 129(1-3): 234-238.

https://doi.org/10.1016/j.jhazmat.2005.08.032

[23] Danish, M., Sulaiman, O., Rafatullah, M., Hashim, R., Ahmad, A. (2010). Kinetics for the removal of paraquat dichloride from aqueous solution by activated date (Phoenix dactylifera) stone carbon. Journal of Dispersion Science and Technology, 31(2): 248-259. https://doi.org/10.1080/01932690903167368

[24] Mojiri, A., Zhou, J.L., Robinson, B., Ohashi, A., et al. (2020). Pesticides in aquatic environments and their removal by adsorption methods. Chemosphere, 253: 126646. https://doi.org/10.1016/j.Chemosphere.2020.126646

[25] Alrefaee, S.H., Aljohani, M., Alkhamis, K., Shaaban, F., El-Desouky, M.G., El-Bindary, A.A., El-Bindary, M.A. (2023). Adsorption and effective removal of organophosphorus pesticides from aqueous solution via novel metal-organic framework: Adsorption isotherms, kinetics, and optimization via Box-Behnken design. Journal of Molecular Liquids, 384: 122206. https://doi.org/10.1016/j.molliq.2023.122206

[26] Yeganeh, M., Charkhloo, E., Sobhi, H.R., Esrafili, A., Gholami, M. (2022). Photocatalytic processes associated with degradation of pesticides in aqueous solutions: Systematic review and meta-analysis. Chemical Engineering Journal, 428: 130081. https://doi.org/10.1016/j.cej.2021.130081

[27] Dolatabadi, M., Ehrampoush, M.H., Pournamdari, M., Ebrahimi, A.A., Fallahzadeh, H., Ahmadzadeh, S. (2023). Simultaneous electrochemical degradation of pesticides from the aqueous environment using Ti/SnO$_2$-Sb$_2$O$_3$/PbO$_2$/Bi electrode; process modeling and mechanism insight. Chemosphere, 311: 137001. https://doi.org/10.1016/j. Chemosphere.2022.137001

[28] He, J., Li, J., Gao, Y., He, X., Hao, G. (2023). Nano-based smart formulations: A potential solution to the hazardous effects of pesticide on the environment. Journal of Hazardous Materials, 456: 131599. https://doi.org/10.1016/j.jhazmat.2023.131599

[29] Zieliński, B., Miądlicki, P., Przepiórski, J. (2022). Development of activated carbon for removal of pesticides from water: Case study. Scientific Reports, 12(1): 20869. https://doi.org/10.1038/s41598-022-25247-6

[30] Ullah, S., Shah, S.S.A., Altaf, M., Hossain, I., et al. (2024). Activated carbon derived from biomass for wastewater treatment: Synthesis, application and future challenges. Journal of Analytical and Applied Pyrolysis, 179: 106480. https://doi.org/10.1016/j.jaap.2024.106480

[31] Malini, K., Selvakumar, D., Kumar, N.S. (2023). Activated carbon from biomass: Preparation, factors improving basicity and surface properties for enhanced CO$_2$ capture capacity-A review. Journal of CO2 Utilization, 67: 102318. https://doi.org/10.1016/j.jcou.2022.102318

[32] Coromina, H.M., Walsh, D.A., Mokaya, R. (2016). Biomass-derived activated carbon with simultaneously enhanced CO$_2$ uptake for both pre and post combustion capture applications. Journal of Materials Chemistry A, 4(1): 280-289. https://doi.org/10.1039/C5TA09202G

[33] Muttil, N., Jagadeesan, S., Chanda, A., Duke, M., Singh, S.K. (2022). Production, types, and applications of activated carbon derived from waste tyres: An overview. Applied Sciences, 13(1): 257. https://doi.org/10.3390/app13010257

[34] Zhu, W., He, J., Wang, Q., Zhang, D., et al. (2024). Activated carbon based on recycled epoxy boards and their adsorption toward Methyl Orange. Polymers, 16(12): 1648. https://doi.org/10.3390/polym16121648

[35] Alrowais, R., Abdel Daiem, M.M., Nasef, B.M., Said, N. (2023). Activated carbon fabricated from biomass for adsorption/bio-adsorption of 2, 4-D and MCPA: Kinetics, isotherms, and artificial neural network modeling. Sustainability, 16(1): 299. https://doi.org/10.3390/su16010299

[36] Harabi, S., Guiza, S., Álvarez-Montero, A., Gómez-Avilés, A., Bagané, M., Belver, C., Bedia, J. (2024). Adsorption of pesticides on activated carbons from peach stones. Processes, 12(1): 238. https://doi.org/10.3390/pr12010238

[37] Bai, X., Quan, B., Kang, C., Zhang, X., et al. (2023). Activated carbon from tea residue as efficient absorbents for environmental pollutant removal from wastewater. Biomass Conversion and Biorefinery, 13(15): 13433-13442. https://doi.org/10.1007/s13399-022-02316-4

[38] Hussain, O.A., Hathout, A.S., Abdel-Mobdy, Y.E., Rashed, M.M., Rahim, E.A., Fouzy, A.S.M. (2023). Preparation and characterization of activated carbon from agricultural wastes and their ability to remove chlorpyrifos from water. Toxicology Reports, 10: 146-154. https://doi.org/10.1016/j.toxrep.2023.01.011

[39] Georgin, J., Pinto, D., Franco, D.S., Schadeck Netto, M., et al. (2022). Improved adsorption of the toxic herbicide diuron using activated carbon obtained from residual cassava biomass (Manihot esculenta). Molecules, 27(21): 7574. https://doi.org/10.3390/molecules27217574

[40] Blachnio, M., Derylo-Marczewska, A., Charmas, B., Zienkiewicz-Strzalka, M., Bogatyrov, V., Galaburda, M. (2020). Activated carbon from agricultural wastes for adsorption of organic pollutants. Molecules, 25(21): 5105. https://doi.org/10.3390/molecules25215105

[41] Pandiarajan, A., Kamaraj, R., Vasudevan, S., Vasudevan, S. (2018). OPAC (orange peel activated carbon) derived from waste orange peel for the adsorption of chlorophenoxyacetic acid herbicides from water: adsorption isotherm, kinetic modelling and thermodynamic studies. Bioresource Technology, 261: 329-341. https://doi.org/10.1016/j.biortech.2018.04.005

[42] Mohammad, S.G., Ahmed, S.M. (2017). Preparation of environmentally friendly activated carbon for removal of pesticide from aqueous media. International Journal of Industrial Chemistry, 8: 121-132. https://doi.org/10.1007/s40090-017-0115-2

[43] Albalasmeh, A.A., Quzaih, M.Z., Gharaibeh, M.A., Rusan, M., et al. (2024). Significance of pyrolytic temperature, application rate and incubation period of biochar in improving hydro-physical properties of calcareous sandy loam soil. Scientific Reports, 14(1): 7012. https://doi.org/10.1038/s41598-024-57755-y

[44] Mahmoud, E.N., Fayed, F.Y., Ibrahim, K.M., Jaafreh, S. (2021). Removal of cadmium, copper, and lead from water using bio-sorbent from treated olive mill solid residue. Environmental Health Insights, 15: 11786302211053176. https://doi.org/10.1177/11786302211053176

[45] Alkhalidi, A., Halaweh, G., Khawaja, M.K. (2023). Recommendations for olive mills waste treatment in hot and dry climate. Journal of the Saudi Society of

Agricultural Sciences, 22(6): 361-373. https://doi.org/10.1016/j.jssas.2023.03.002

[46] Nahar Myyas, R.E., Tostado-Véliz, M., Gómez-González, M., Jurado, F. (2023). Review of bioenergy potential in Jordan. Energies, 16(3): 1393. https://doi.org/10.3390/en16031393

[47] Al-Khalid, T.T., Haimour, N.M., Sayed, S.A., Akash, B.A. (1998). Activation of olive-seed waste residue using CO_2 in a fluidized-bed reactor. Fuel Processing Technology, 57(1): 55-64. https://doi.org/10.1016/S0378-3820(98)00070-8

[48] Rahman, M.S., Sathasivam, K.V. (2015). Heavy metal adsorption onto Kappaphycus sp. from aqueous solutions: the use of error functions for validation of isotherm and kinetics models. BioMed Research International, 2015(1): 126298. https://doi.org/10.1155/2015/126298

[49] Foo, K.Y., Hameed, B.H. (2010). Insights into the modeling of adsorption isotherm systems. Chemical Engineering Journal, 156(1): 2-10. https://doi.org/10.1016/j.cej.2009.09.013

[50] Chen, X. (2015). Modeling of experimental adsorption isotherm data. Information, 6(1): 14-22. https://doi.org/10.3390/info6010014

[51] Mansoor, S.J., Abbasitabar, F. (2020). Adsorption behavior of Fe (II) and Fe (III) ions on polyaniline coated sawdust: batch and fixed-bed studies. Acta Chimica Slovenica, 67(1): 36-46. https://doi.org/10.17344/acsi.2019.5121

[52] Lian, L., Guo, L., Guo, C. (2009). Adsorption of Congo red from aqueous solutions onto Ca-bentonite. Journal of Hazardous Materials, 161(1): 126-131. https://doi.org/10.1016/j.jhazmat.2008.03.063

[53] Itodo, A.U., Itodo, H.U., Gafar, M.K. (2010). Estimation of specific surface area using Langmuir isotherm method. Journal of Applied Sciences and Environmental Management, 14(4): 141-145. https://doi.org/10.4314/jasem.v14i4.63287

[54] Zagorny, M., Lobunets, T., Pozniy, A., Ragulya, A. (2013). Mesoporous structure and photocatalytic activity of doped polyanilines. Journal of Chemistry and Chemical Engineering, 7(12): 1121-1126. https://doi.org/10.17265/1934-7375/2013.12.003

[55] Yadav, M., Jadeja, R., Thakore, S. (2022). An ecofriendly approach for methylene blue and lead (II) adsorption onto functionalized Citrus limetta bioadsorbent. Environmental Processes, 9(2): 27. https://doi.org/10.1007/s40710-022-00583-x

[56] Istiqomah, N.I., Budianti, S.I., Cuana, R., Puspitarum, D.L., Mahardhika, L.J., Suharyadi, E. (2024). Magnetically separable and reusable Fe_3O_4/chitosan nanocomposites green synthesized utilizing Moringa oleifera extract for rapid photocatalytic degradation of methylene blue. Results in Chemistry, 7: 101245. https://doi.org/10.1016/j.rechem.2023.101245

[57] Alslaibi, T.M., Abustan, I., Ahmad, M.A., Foul, A.A. (2013). A review: Production of activated carbon from agricultural byproducts via conventional and microwave heating. Journal of Chemical Technology & Biotechnology, 88(7): 1183-1190. https://doi.org/10.1002/jctb.4028

[58] Zhang, T., Walawender, W.P., Fan, L.T., Fan, M., Daugaard, D., Brown, R.C. (2004). Preparation of activated carbon from forest and agricultural residues through CO_2 activation. Chemical Engineering Journal, 105(1-2): 53-59. https://doi.org/10.1016/j.cej.2004.06.011

[59] Zhao, Y., Yan, Y., Jiang, Y., Cao, Y., et al. (2024). Release pattern of light aromatic hydrocarbons during the biomass roasting process. Molecules, 29(6): 1188. https://doi.org/10.3390/molecules29061188

[60] Wang, X., Li, D., Li, W., Peng, J., et al. (2013). Optimization of mesoporous activated carbon from coconut shells by chemical activation with phosphoric acid. BioResources, 8(4): 6184-6195. https://doi.org/10.15376/biores.8.4.6184-6195

[61] Tsai, C.H., Tsai, W.T. (2023). Optimization of physical activation process by CO2 for activated carbon preparation from Honduras Mahogany pod husk. Materials, 16(19): 6558. https://doi.org/10.3390/ma16196558

[62] Yi, N., Wu, Y., Fan, L., Hu, S. (2019). Remediating Cd-contaminated soils using natural and chitosan-introduced zeolite, bentonite, and activated carbon. Polish Journal of Environmental Studies, 28(3): 1461-1468. https://doi.org/10.15244/pjoes/89577

[63] Inel, O., Tümsek, F. (2000). The measurement of surface areas of some silicates by solution adsorption. Turkish Journal of Chemistry, 24(1): 9-19.

[64] Otalvaro, J.O., Brigante, M. (2018). Interaction of pesticides with natural and synthetic solids. Evaluation in dynamic and equilibrium conditions. Environmental Science and Pollution Research, 25: 6707-6719. https://doi.org/10.1007/s11356-017-1020-0

[65] Sanchez-Martin, M.J., Rodriguez-Cruz, M.S., Andrades, M.S., Sanchez-Camazano, M. (2006). Efficiency of different clay minerals modified with a cationic surfactant in the adsorption of pesticides: Influence of clay type and pesticide hydrophobicity. Applied Clay Science, 31(3-4): 216-228. https://doi.org/10.1016/j.clay.2005.07.008

[66] Ewis, D., Ba-Abbad, M.M., Benamor, A., El-Naas, M.H. (2022). Adsorption of organic water pollutants by clays and clay minerals composites: A comprehensive review. Applied Clay Science, 229: 106686. https://doi.org/10.1016/j.clay.2022.106686

[67] Cougnaud, A., Faur, C., Le Cloirec, P. (2005). Removal of pesticides from aqueous solution: quantitative relationship between activated carbon characteristics and adsorption properties. Environmental Technology, 26(8): 857-866. https://doi.org/10.1080/09593332608618497

[68] Faur, C., Métivier-Pignon, H., Le Cloirec, P. (2005). Multicomponent adsorption of pesticides onto activated carbon fibers. Adsorption, 11: 479-490. https://doi.org/10.1007/s10450-005-5607-2

[69] Saha, A., Gajbhiye, V.T., Gupta, S., Kumar, R., Ghosh, R.K. (2014). Simultaneous removal of pesticides from water by rice husk ash: batch and column studies. Water Environment Research, 86(11): 2176-2185. https://doi.org/10.2175/106143014X14062131178358

[70] Shaban, M., Abukhadra, M.R. (2017). Geochemical evaluation and environmental application of Yemeni natural zeolite as sorbent for Cd 2+ from solution: kinetic modeling, equilibrium studies, and statistical optimization. Environmental Earth Sciences, 76: 310. https://doi.org/10.1007/s12665-017-6636-3

[71] Sadeghi, M., Yekta, S., Ghaedi, H., Babanezhad, E.

(2016). Effective removal of radioactive 90 Sr by CuO NPs/Ag-clinoptilolite zeolite composite adsorbent from water sample: Isotherm, kinetic and thermodynamic reactions study. International Journal of Industrial Chemistry, 7: 315-331. https://doi.org/10.1007/s40090-016-0092-x

[72] Iqajtaoune, A., Taibi, M.H., Saufi, H., Aouan, B., Boudad, L. (2024). Enhanced removal of methylene blue and procion deep red H-EXL dyes from aqueous environments by modified-bentonite: Isotherm, kinetic, and thermodynamic. Desalination and Water Treatment, 320: 100607. https://doi.org/10.1016/j.dwt.2024.100607